Discrete lossless convexification for pointing constraints

Dayou Luo[1], Fabio Spada[2], Behçet Açıkmeşe[3]

***Abstract*—Discrete Lossless Convexification (DLCvx) formulates a convex relaxation for a specific class of discrete-time non-convex optimal control problems. It establishes sufficient conditions under which the solution of the relaxed problem satisfies the original non-convex constraints at specified time grid points. Furthermore, it provides an upper bound on the number of time grid points where these sufficient conditions may not hold, and thus the original constraints could be violated. This paper extends DLCvx to problems with control pointing constraints. Additionally, it introduces a novel DLCvx formulation for mixed-integer optimal control problems in which the control is either inactive or constrained within an annular sector. This formulation broadens the feasible space for problems with pointing constraints. A numerical example is provided to illustrate its application.**

***Index Terms*—Lossless convexification, convex optimization, pointing constraints, computational guidance**

I. Introduction

IN THE most recent years, convex optimization has become the capstone of computational guidance and control strategies for autonomous systems; convergence to globally optimal points and polynomial-time complexity constitute its strengths [1]. In this context, a few non-convex Optimal Control Problems (OCPs) can be *relaxed* to provably-equivalent convex OCPs by substituting the non-convex constraints with their convex counterparts. The relaxed problem can then be solved to global optimality while preserving the satisfaction of the original non-convex constraints. This relaxation technique is therefore referred to as Lossless Convexification (LCvx).

LCvx has been successfully applied to problems with annular control constraints [2]–[4], pointing constraints [5] and linear and quadratic state constraints [6], [7]. More recent studies tackle non-convexities of mixed-integer (MI) nature: controls can be constrained to semi-continuous sets by relaxing the MI constraint of an optimal multiplexing problem [8]; quantized controls can be enforced leveraging non-smooth convex hulls [9], [10]; interestingly, quantized controls for the special scenario of relative-orbit control can be obtained by leveraging a sum-of-absolute-values objective function, resulting in an efficient linear programming formulation [11]. The interested reader is referred to [12] for an exhaustive analysis of the current status of LCvx.

The previously mentioned examples establish the relationship between the original Continuous-Time (CT) non-convex OCP and its convex relaxation, but only within the CT domain. When the convex CT-OCP is later *discretized* into a Discrete-Time (DT) OCP for practical computation, the existing theoretical discussions of LCvx on CT-OCP do not ensure that the solution of the DT convex relaxation satisfies the original non-convex constraints. As a result, the LCvx approach remains incomplete in the DT setting.

To address this issue, [13] provides a comprehensive analysis of the relationship between non-convex and convex DT-OCPs by proposing the Discrete LCvx (DLCvx) method. Specifically, DLCvx works directly on the DT non-convex problem and its convex relaxation. It offers a tight upper bound on the number of time grid points where the solution of the convex relaxation violates the original non-convex constraints. Unlike the CT version, DLCvx uses finite-dimensional tools such as convex analysis and linear algebra to establish its theoretical results. This distinction provides a new perspective on understanding the LCvx technique and opens up possibilities for designing novel relaxations.

The present work extends the DLCvx method to solve Optimal Control Problems (OCPs) for Linear Time-Invariant (LTI) systems characterized by control pointing and semi-continuous control magnitude constraints. The former ensures acceptable vehicle orientation during maneuvers, while the latter models dual-mode control, where the control is either null or of finite, bounded magnitude. Both types of constraints are common in aerospace systems control. A continuous-time LCvx formulation exists for the first type of problem, while our formulation for the second type has not appeared in previous research. The contributions of this paper include a) a new pointing constraint that accommodates semi-continuous control magnitude, enabling dual-mode control; b) theoretical guarantees of DLCvx for both formulations, which include sufficient conditions for the solution of the convex relaxation to satisfy the original non-convex constraints at specified time grid points, as well as a finite upper bound on the number of non-convex constraint violations over the full control horizon.

The remainder of the work is organized as follows: the analyzed problems, along with their relaxations, are formulated in Section II. Section III provides the theoretical guarantees for the considered DLCvx method. Section IV presents and solves an application example, showcasing the results for the two described formulations. Finally, conclusions are drawn in Section V.

Notation: The set of integers $\{a, a+1, \ldots, b\}$ is denoted by $[a, b]_{\mathbb{N}}$. $\mathbb{R}$, $\mathbb{R}^n$ and $\mathbb{R}^{n\times m}$ are respectively the set of real numbers, the set of $n-$dimensional vectors, and the set of real $n \times m$ matrices. The rank of a matrix A is denoted by $\mathrm{rank}(A)$, and the Euclidean norm of a vector by $\|\cdot\|$. For matrices $A_1, A_2, \ldots, A_n$ with the same number of rows, their

[1]Ph.D. Candidate, Department of Applied Mathematics, University of Washington, Seattle, WA 98195. dayoul@uw.edu

[2]Ph.D. Student, William E. Boeing Department of Aeronautics and Astronautics, University of Washington, Seattle, WA 98195. fspada46@uw.edu

[3]Professor, William E. Boeing Department of Aeronautics and Astronautics, University of Washington, Seattle, WA 98195. behcet@uw.edu

horizontal concatenation is denoted as $[A_1, A_2, \ldots, A_n]$. The gradient of a function H with respect to variables a and b is written as $\nabla H(a,b)$. The d-dimensional interval $[a,b]^d$ is defined as $\{\mathbf{x} \in \mathbb{R}^d \mid a \le x_i \le b,\ i=1,2,\ldots,d\}$. We denote the identity matrix by $\boldsymbol{I}$ and the zero matrix by $\mathbf{0}$.

II. Problem formulation

This paper addresses two types of lossless convexification for non-convex optimal control problems with pointing constraints. Let us define the two non-convex optimal control problems. The first problem features classical pointing constraints [5]:

Problem 1 (P1):

$$\begin{array}{ll} \underset{x,u}{\text{minimize}} & m\left(x_{N+1}\right)+\sum_{i=1}^{N} l_i\left(\|u_i\|\right) \\ \text{subject to} & \left|\begin{array}{l} \left.\begin{array}{l} x_{i+1}=Ax_i+Bu_i+w_i \\ \rho_{\min} \le \|u_i\| \le \rho_{\max} \\ \xi^\top u_i \ge \gamma\|u_i\| \end{array}\right| \forall i \in [1,N]_{\mathbb{N}} \\ x_1 = x_{\text{init}}, \quad G\left(x_{N+1}\right)=0 \end{array}\right. \end{array}$$

with the following solution variables:

$$\begin{aligned} x &= \{x_1, x_2, \cdots, x_{N+1}\},\ x_i \in \mathbb{R}^{n_x} \text{ for } i \in [1, N+1]_{\mathbb{N}} \\ u &= \{u_1, u_2, \cdots, u_N\},\ u_i \ \in \mathbb{R}^{n_u} \text{ for } i \in [1,N]_{\mathbb{N}} \end{aligned}$$

where x_i, u_i and $w_i \in \mathbb{R}^{n_x}$ are respectively the state, the control input and external force at time step i. The cost functions $m\colon \mathbb{R}^{n_x} \to \mathbb{R}$ and $l_i\colon \mathbb{R} \to \mathbb{R}$ for $i \in [1,N]_{\mathbb{N}}$ are convex C^1 smooth functions, defining the terminal state cost and step-wise control cost. $G\colon \mathbb{R}^{n_x} \to \mathbb{R}^{n_G}$ is an affine map characterizing the boundary condition of the state trajectory. The system dynamics are defined by constant matrices $A \in \mathbb{R}^{n_x \times n_x}$ and $B \in \mathbb{R}^{n_x \times n_u}$, with fixed initial state $x_{\text{init}} \in \mathbb{R}^{n_x}$. The constants $\rho_{\min}, \rho_{\max} \in \mathbb{R}$ bound the control input norm. The pointing constraint $\xi^\top u_i \ge \gamma\|u_i\|$ restricts the angle between u_i and a fixed unit vector ξ, with constant $\gamma > 0$. Additionally, l_i are monotonically increasing functions on the interval $[\rho_{\min}, \infty)$.

The second problem allows null control input, as follows.

Problem 2 (P2):

$$\begin{array}{ll} \underset{x,u,\theta}{\text{minimize}} & m\left(x_{N+1}\right)+\sum_{i=1}^{N} l_i\left(\max(\|u_i\|, \rho_{\min})\right) \\ \text{subject to} & \left|\begin{array}{l} \left.\begin{array}{l} x_{i+1}=Ax_i+Bu_i+w_i \\ \theta_i\rho_{\min} \le \|u_i\| \le \theta_i\rho_{\max} \\ \xi^\top u_i \ge \gamma\|u_i\| \\ \theta_i \in \{0,1\}\ , u_i \in \mathbb{R}^2 \end{array}\right| \forall i \in [1,N]_{\mathbb{N}} \\ x_1 = x_{\text{init}}, \quad G\left(x_{N+1}\right)=0 \end{array}\right. \end{array}$$

The key difference between $P1$ and $P2$ is the introduction of a switching variable $\theta_i \in \{0,1\}$. Each θ_i represents a control mode: $\theta_i = 1$ indicates that the control input u_i is active and bounded within $[\rho_{\min}, \rho_{\max}]$, while $\theta_i = 0$ indicates that u_i is inactive and set to zero. This formulation is particularly useful for representing on-off control systems and extends the feasible region of $P1$. The objective function uses $l_i\left(\max(\|u_i\|, \rho_{\min})\right)$, which serves as an approximation of $l_i\left(\|u_i\|\right)$. The latter form cannot be addressed using our current method and is left for future research.

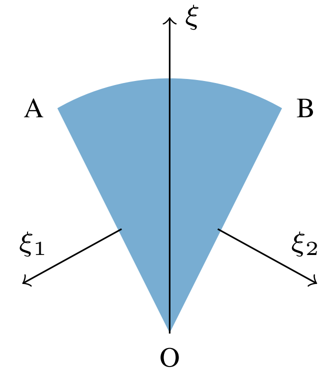

Fig. 1: Pointing constraint for $P4$

Furthermore, $u_i \in \mathbb{R}^2$ for $P2$, whereas dimension of u_i is not prescribed in $P1$. We will later demonstrate why LCvx is effective in $\mathbb{R}^2$ but may fail in higher dimensions.

Both $P1$ and $P2$ are inherently non-convex, making them difficult to solve using standard numerical methods. To overcome this, we formulate two convex relaxed versions of $P1$ and $P2$, which yield solutions satisfying the constraints of $P1$ and $P2$ at almost all temporal grid points.

For $P1$, we apply the standard LCvx for pointing constraints [5]. The resulting convexified problem reads:

Problem 3 (P3):

$$\begin{array}{ll} \underset{x,u,\sigma}{\text{minimize}} & m\left(x_{N+1}\right)+\sum_{i=1}^{N} l_i\left(\sigma_i\right) \\ \text{subject to} & \left|\begin{array}{l} \left.\begin{array}{l} x_{i+1}=Ax_i+Bu_i+w_i \\ \rho_{\min} \le \sigma_i \le \rho_{\max} \\ \xi^\top u_i \ge \gamma\sigma_i \\ \sigma_i \ge \|u_i\| \end{array}\right| \forall i \in [1,N]_{\mathbb{N}} \\ x_1 = x_{\text{init}}, \quad G\left(x_{N+1}\right)=0 \end{array}\right. \end{array}$$

Here, $\sigma_i \in \mathbb{R}$ for all i, and we define $\sigma = \{\sigma_1, \sigma_2, \cdots, \sigma_N\}$. All other variables and coefficients are defined as in $P1$.

$P2$ is a MI optimization problem that cannot be directly solved using continuous optimization techniques. To address this, we recast $P2$ as follows

Problem 4 (P4):

$$\begin{array}{ll} \underset{x,u,\sigma}{\text{minimize}} & m\left(x_{N+1}\right)+\sum_{i=1}^{N} l_i\left(\sigma_i\right) \\ \text{subject to} & \left|\begin{array}{l} \left.\begin{array}{l} x_{i+1}=Ax_i+Bu_i+w_i \\ \rho_{\min} \le \sigma_i \le \rho_{\max} \\ \xi^\top u_i \ge \gamma\|u_i\| \\ \sigma_i \ge \|u_i\|,\ u_i \in \mathbb{R}^2 \end{array}\right| \forall i \in [1,N]_{\mathbb{N}} \\ x_1 = x_{\text{init}}, \quad G\left(x_{N+1}\right)=0 \end{array}\right. \end{array}$$

The feasible region for u_i, given a specific value of σ_i, is a sector-shaped region, as shown in Figure 1. The angle $\angle AOB$ varies between 0 and 180 degrees, depending on γ. Let ξ_1 and ξ_2 denote the unit vector respectively perpendicular to the boundaries OA and OB.

$P3$ and $P4$ can be consistently reformulated as:

Problem 5 (P5):

$$\begin{aligned}\min_{x,u,\sigma} \quad & m\left(x_{N+1}\right)+\textstyle\sum_{i=1}^{N}\left[l_i\left(\sigma_i\right)+I_V\left(u_i,\sigma_i\right)\right] \\ \text{s.t.} \quad & x_{i+1}=Ax_i+Bu_i+w_i, \quad \forall i\in[1,N]_{\mathbb{N}} \\ & x_1=x_{\text{init}}, \quad G\left(x_{N+1}\right)=0.\end{aligned}$$

where the *indicator function* $I_V(u,\sigma)$ of the convex set V is 0 for $(u,\sigma)\in V$ and $+\infty$ otherwise [14]. The sets V for $P3$ are defined as:

$$V_{P3}=\{(\bar{u},\bar{\sigma})\in\mathbb{R}^{n_u}\times\mathbb{R} \mid \rho_{\min}\le\bar{\sigma}\le\rho_{\max}, \\ \xi^\top\bar{u}\ge\gamma\bar{\sigma}, \ \ \bar{\sigma}\ge\|\bar{u}\|\},$$

$$V_{P4}=\{(\bar{u},\bar{\sigma})\in\mathbb{R}^{2}\times\mathbb{R} \mid \rho_{\min}\le\bar{\sigma}\le\rho_{\max}, \\ \xi^\top\bar{u}\ge\gamma\|\bar{u}\|, \ \ \bar{\sigma}\ge\|\bar{u}\|\}.$$

After removing redundant boundary conditions, the affine equality constraints can be combined into a single affine constraint $H(x,u)=0$, with Jacobian ∇H. We then make the following assumption:

Assumption 1. *∇H is full rank.*

We define LCvx as *valid* for $P3$ at time grid point i if the optimal control u_i satisfies the control constraints in $P1$. Similarly, LCvx is *valid* for $P4$ at time grid point i if the optimal solution u_i satisfies the control constraints in $P2$ for some $\theta_i\in\{0,1\}$.

Referring to the control at a generic time grid point i as $(\bar{u},\bar{\sigma})$, we now provide a sufficient condition to ensure the validity of LCvx for $P3$ and $P4$ at i.

Lemma 1 (Sufficient Condition for LCvx)**.** *For a point $(\bar{u},\bar{\sigma})\in V_{P3}$, $\bar{u}$ satisfies the constraints for controls in Problem $P1$ if*

$$N_{V_{P3}}(\bar{u},\bar{\sigma})\nsubseteq\{\lambda\xi\mid\lambda\in\mathbb{R}\}.$$

Here $N_{V_{P3}}(\bar{u},\bar{\sigma})$ is the normal cone [14, Chapter 2.1] of V_{P3} at point $(\bar{u},\bar{\sigma})$. Similarly, for a point $(\bar{u},\bar{\sigma})\in V_{P4}$, the constraints for controls in Problem $P2$ are satisfied by $\bar{u}$ with some $\theta\in\{0,1\}$ if

$$N_{V_{P4}}(\bar{u},\bar{\sigma})\nsubseteq\{\lambda\xi_1\mid\lambda\in\mathbb{R}\}\cup\{\lambda\xi_2\mid\lambda\in\mathbb{R}\}.$$

Proof. We prove the lemma for P_4 by contraposition. There are two scenarios where the constraints in P_2 can be violated: (1) $(\bar{u},\bar{\sigma})$ is in the interior of V_{P4}, or (2) $(\bar{u},\bar{\sigma})$ lies on the line segment OA or OB, but not at points O,A, or B.

If (1) is verified, then $N_{V_{P4}}(\bar{u},\bar{\sigma})=\{0\}$ [15, Corollary 6.44]. If (2) is verified, then

$$N_{V_{P4}}=\{\lambda\xi_1\mid\lambda\in\mathbb{R}_+\} \quad \text{or} \quad N_{V_{P4}}=\{\lambda\xi_2\mid\lambda\in\mathbb{R}_+\}.$$

Thus, in either case,

$$N_{V_{P4}}(\bar{u},\bar{\sigma})\subseteq\{\lambda\xi_1\mid\lambda\in\mathbb{R}\}\cup\{\lambda\xi_2\mid\lambda\in\mathbb{R}\},$$

which contradicts the condition of the lemma.
Proof for P_3 is analogous. ☐

III. Theoretical Guarantee for LCvx Validity

In this section, we formally establish the validity of LCvx for the solutions of $P3$ and $P4$ and derive an upper bound on the number of temporal grid points where the optimal solutions to $P3$ and $P4$ may violate the non-convex constraints of $P1$ and $P2$ respectively.

We begin by assuming Slater's condition holds for $P5$, which also holds for both $P3$ and $P4$.

Assumption 2 (Slater's Condition)**.** *For $P5$, there exists a combination of (x,u,σ) such that (u_i,σ_i) lies in the interior of set V for all i and (x_i,u_i) satisfies all affine constraints.*

Slater's condition ensures the validity of the following theorem for the Lagrangian of $P5$, which is defined as:

$$\begin{aligned}L(x,u,\sigma;\eta,\mu_1,\mu_2):=&\,m\left(x_{N+1}\right)+\sum_{i=1}^{N}\left[l_i\left(\sigma_i\right)+I_V\left(u_i,\sigma_i\right)\right] \\ &+\sum_{i=1}^{N}\eta_i^\top\left(-x_{i+1}+Ax_i+Bu_i+w_i\right) \\ &+\mu_1^\top\left(x_1-x_{\text{init}}\right)+\mu_2^\top G\left(x_{N+1}\right).\end{aligned}$$

Here the dual variables are defined as $\eta_i\in\mathbb{R}^{n_x}$ for $i=1,2,\cdots,N$, and they are concatenated to form the vector $\eta=[\eta_1^\top,\eta_2^\top,\cdots,\eta_N^\top]^\top\in\mathbb{R}^{n_xN}$. Additionally, $\mu_1\in\mathbb{R}^{n_x}$ and $\mu_2\in\mathbb{R}^{n_G}$ are the dual variables associated with the initial state and boundary constraints, respectively.

Theorem 1. *Given a solution (x^*,u^*,σ^*) of P5 and Assumption 2, there exist dual variables (η^*,μ_1^*,μ_2^*) such that*

$$(x^*,u^*,\sigma^*)=\arg\min_{x,u,\sigma}L\left(x,u,\sigma;\eta^*,\mu_1^*,\mu_2^*\right).$$

Proof. This follows directly from [16, Theorem 9.4, 9.8 and 9.14]. ☐

From equation (1), we derive:

$$\begin{aligned}\sigma^*&=\arg\min_{\sigma}L\left(x^*,u^*,\sigma;\eta^*,\mu_1^*,\mu_2^*\right), \\ u^*&=\arg\min_{u}L\left(x^*,u,\sigma^*;\eta^*,\mu_1^*,\mu_2^*\right), \\ x^*&=\arg\min_{x}L\left(x,u^*,\sigma^*;\eta^*,\mu_1^*,\mu_2^*\right).\end{aligned}$$

Since in the Lagrangian L, u_i only appears in terms $I_V(u_i,\sigma_i)$ and $\eta_i^\top Bu_i$, we have the following equation which characterizes the relationship between u_i^* and σ_i^*:

$$\begin{aligned}u_i^*&=\arg\min_{u_i}I_V\left(u_i,\sigma_i^*\right)+\eta_i^{*\top}Bu_i \\ &=\arg\min_{u_i}I_{V\left(\sigma_i^*\right)}\left(u_i\right)+\eta_i^{*\top}Bu_i,\end{aligned}$$

where the set $V(\sigma_i^*)$ is defined as

$$V(\sigma_i^*)=\{\bar{u}\in\mathbb{R}^{n_u} \mid (\bar{u},\sigma_i^*)\in V\}.$$

Specifically, we present the following theorem from [13, Theorem 10], with the proof provided for completeness.

Theorem 2. *Under Assumptions 2 for $P5$, we have $\eta_i^*=A^{\top(N-i)}\eta_N$ and $-B^\top\eta_i^*\in N_{V\left(\sigma_i^*\right)}\left(u_i^*\right)$.*

Proof. Given that the right-hand side function of equation (III) is convex in u_i and u_i^* is a minimizer of this convex function, it follows that [14, Proposition 2.1.2] $-B^\top \eta_i^* \in N_{V(\sigma_i^*)}(u_i^*)$, where $N_{V(\sigma_i^*)}(u_i)$ denotes the normal cone of the set $V(\sigma_i^*)$ at point u_i^*.

For the evolution of η_i, considering equation (III), we take the partial derivative of L with respect to x_i for all i, yielding:

$$\begin{aligned} x_{N+1}: &\quad \nabla m(x_{N+1}) + \mu_2^\top \nabla G(x_{N+1}) = \eta_N^*, \\ x_i: &\quad \eta_i^{*\top} A - \eta_{i-1}^{*\top} = 0, \\ x_1: &\quad \mu_1^\top + \eta_1^{*\top} A = 0. \end{aligned}$$

Thus, iteratively applying (1) leads to $\eta_i^* = A^{\top(N-i)}\eta_N^*$. □

Hence, we have the following sufficient condition for LCvx for a specific grid point i.

Theorem 3. *LCvx is valid for $P3$ at time grid point i if*

$$-B^\top \eta_i^* \neq \lambda\xi, \quad \textit{for all } \lambda \in \mathbb{R}.$$

Similarly, LCvx is valid for $P4$ at time grid point i if

$$-B^\top \eta_i^* \neq \lambda\xi_1 \ \wedge \ -B^\top \eta_i^* \neq \lambda\xi_2, \quad \textit{for all } \lambda \in \mathbb{R}.$$

Proof. This theorem holds as a direct consequence of Lemma 1 and Theorem 2. □

We are now ready to analyze the validity of LCvx for the whole trajectory of $P3$ and $P4$. To proceed, we first introduce the definition of controllability and specify the controllability assumption for $P3$ and $P4$.

Definition 4 (Controllability). *The matrix pair (A, B), where $A \in \mathbb{R}^{n_x \times n_x}$ and $B \in \mathbb{R}^{n_x \times n_u}$, is said to be controllable if the controllability matrix*

$$\mathcal{C} = \begin{bmatrix} B & AB & A^2B & \cdots & A^{n_x-1}B \end{bmatrix}$$

has full row rank, i.e. $\operatorname{rank}(\mathcal{C}) = n_x$.

We require the following controllability condition for $P3$:

Assumption 3 (Controllability for $P3$). *Let $M \in \mathbb{R}^{n_u \times (n_u-1)}$ be a matrix whose columns form a basis for the orthogonal complement of vector ξ in $P3$. For matrices A and B in $P3$, we require the matrix pair $\{A, BM\}$ to be controllable.*

Similarly, we need the following assumption for $P4$:

Assumption 4 (Controllability for $P4$). *For problem 4, let $w_1 \in \mathbb{R}^2$ and $w_2 \in \mathbb{R}^2$ be two unit vectors such that $\xi_1^\top w_1 = 0$ and $\xi_2^\top w_2 = 0$ in $P4$. For matrices A and B, we require both matrix pairs $\{A, Bw_1\}$ and $\{A, Bw_2\}$ to be controllable.*

We also need the transversality assumption for both Problem 3 and Problem 4.

Assumption 5 (Transversality). *For both $P3$ and $P4$, the dual variable η_N must satisfy: $\eta_N \neq 0$.*

Remark 5. *Assumption 5 may not hold if the control horizon is excessively long, resulting in a convexified problem's optimal solution in which the input magnitude violates the non-convex input constraints throughout the entire trajectory. In such cases, a bisection search method can be applied iteratively to reduce the control horizon until Assumption 5 is satisfied. For further details, we refer the interested reader to [13].*

Given these assumptions, we have the following theorem for $P3$.

Theorem 6. *Under Assumptions 2, 3, and 5, the optimal solution for $P3$ does not violate LCvx at the last n_x temporal grid points.*

Proof. Under Assumption 3, the left null space of the matrix

$$S = \begin{bmatrix} BM & ABM & \cdots & A^{n_x-1}BM \end{bmatrix}$$

contains only the zero vector. Consequently, Assumption 5 guarantees that $\eta_N^\top S$ is non-zero, which implies that there exists a nonnegative integer $i < n_x$ such that $\eta_N^\top A^i BM \neq 0$. Since the column space of M is orthogonal to ξ, it follows that $\eta_N^\top A^i B$ is neither parallel to ξ nor zero. Furthermore, by Theorem 3, we have $\eta_N^\top A^i B = \eta_{N-i}^\top B$.

Therefore, Theorem 3 ensures that LCvx is valid at the $N-i$th time grid point. □

The remainder of this chapter extends Theorem 6 to cover the entire trajectory of $P3$ and derives the corresponding result for $P4$. Importantly, controllability alone is insufficient for this generalization. Counterexamples for problems without pointing constraints exist [13]. To address this, we introduce a perturbation to the matrix in the dynamic system (iterative linear constraints), as defined in [13, Definition 16]. This perturbation adjusts the matrix's eigenvalues while preserving its Jordan form.

Definition 7. *For matrix $A \in \mathbb{R}^{n_x \times n_x}$, let matrix A's Jordan form be*

$$A = Q^{-1} J Q.$$

Assuming A has d distinct eigenvalues, we set these eigenvalues as $(\lambda_1, \cdots, \lambda_d)$. Define $\tilde{A}(q)$ as a perturbation of A with respect to a vector $q = (q_1, q_2, \cdots, q_d) \in \mathbb{R}^d$ if:

- *$\tilde{A}(q) = Q^{-1}\tilde{J}(q)Q$, where $\tilde{J}(q)$ is a Jordan matrix with the same structure as J, but with different eigenvalues.*
- *$\tilde{A}(q)$ has d distinct eigenvalues such that $(\tilde{\lambda}_1, \cdots, \tilde{\lambda}_d) = (\lambda_1, \lambda_2, \cdots, \lambda_d) + (q_1, q_2, \cdots, q_d)$.*
- *The index of Jordan blocks in $\tilde{J}(q)$ corresponding to $\tilde{\lambda}_i$ remains the same as in J corresponding to λ_i.*

After presenting the perturbation theorem, we demonstrate that all previously satisfied assumptions for $P3$ and $P4$ continue to hold for the perturbed problem when the matrix A in the dynamics is perturbed.

Lemma 2 ([13, Lemma 17]). *If Assumptions 1, 2, 3, 4, 5 hold, then there exists $\epsilon > 0$ such that for any q satisfying $\|q\| \leq \epsilon$, Assumptions 1, 2, 3, 4, 5 remain valid for the perturbed P3, P4, and P5, wherein matrix A is replaced by its perturbed counterpart $A(q)$.*

Additionally, the following lemma holds:

Lemma 3 ([13, Theorem 20]). *Consider a generic controllable matrix pair $(\bar{A}, \bar{B}) \in (\mathbb{R}^{n_x \times n_x}, \mathbb{R}^{n_x \times n_u})$. Let $\tilde{A}(q)$*

denote the perturbed matrix of $\bar{A}$ with respect to a vector $q \in \mathbb{R}^d$, where q is generated by a uniform distribution over a d-dimensional unit cube, i.e., $q \in [-\frac{1}{2}, \frac{1}{2}]^d$. Then, the matrix

$$\begin{bmatrix} \tilde{A}(q)^{N-P_1}\bar{B} & \tilde{A}(q)^{N-P_2}\bar{B} & \cdots & \tilde{A}(q)^{N-P_{n_x}}\bar{B} \end{bmatrix}$$

has full row rank with probability one. Here, $P_1, P_2, \cdots, P_{n_x} \in [1, N]_{\mathbb{N}}$ are distinct integers representing temporal grid points.

We are now ready to present our main result:

Theorem 8. *Under Assumptions 1, 2, and 5, the following holds for both $P3$ and $P4$:*

If Assumption 3 holds for $P3$ and Assumption 4 for $P4$, then there exists an $\epsilon > 0$ such that for a random vector $q \in \mathbb{R}^d$ uniformly distributed over $[-\frac{\epsilon}{2}, \frac{\epsilon}{2}]^d$, the probability that the optimal trajectory of the perturbed system—obtained by replacing the dynamics matrix A with its perturbed version $\tilde{A}(q)$—violates the non-convex constraints in $P1$ at more than $n_x - 1$ points for $P3$, or in $P2$ at more than $2n_x - 2$ points for $P4$, is zero.

Proof. We first consider the statement for $P3$. Let $\{P_1, P_2, \ldots, P_{n_x}\}$ be any n_x distinct integers selected from the set $[1, N]_{\mathbb{N}}$. By Lemma 3, the controllability of $\{A, BM\}$ ensures that the matrix

$$\begin{bmatrix} \tilde{A}(q)^{N-P_1}BM & \tilde{A}(q)^{N-P_2}BM & \cdots & \tilde{A}(q)^{N-P_{n_x}}BM \end{bmatrix}$$

has full row rank with probability one. Using the same reasoning as in Theorem 6 and under the assumptions verified by Lemma 2 for sufficiently small ϵ, we conclude that, for any set of n_x distinct temporal grid points, LCvx is valid at least at one of these grids with probability one. Consequently, since there are only a finite number of ways to choose n_x distinct temporal grid points, LCvx can be violated at most at $n_x - 1$ temporal grid points along the entire trajectory with probability one.

Now we consider the statement for $P4$. Using a similar argument as for $P3$, the probability of having n_x temporal grid points where the control lands on line segment OA without being at points O or A is zero. Likewise, the probability of having n_x temporal grid points where the control lands on line segment OB without being at points O or B is also zero. Therefore, for the entire trajectory, LCvx can be violated at most at $2n_x - 2$ temporal grid points with probability one. □

Remark 9. *The LCvx method in $P3$ and $P4$ follows a pattern: we identify problematic regions on the control boundary that invalidate LCvx and show that the dual variable associated with the system dynamics stays within the normal cones of the control. Since these normal cones consist of single-ray directions, the control avoids these regions unless the dual variable aligns with these rays. Using controllability, we demonstrate that this alignment occurs at most $n_x - 1$ times, limiting control entries into these regions.*

For higher-dimensional $P4$ cases, however, problematic regions—such as cone surfaces in $\mathbb{R}^3$—contain infinitely many normal directions, making single-direction avoidance insufficient. Polyhedral cones can then limit the critical directions. In practice, LCvx violations for the pointing constraint in $\mathbb{R}^3$ are minimal, as illustrated in the next section.

IV. Numerical analyses

Let us consider the flight of a quadrotor, landing at a given position $\bar{r}_f \in \mathbb{R}^3$ with fixed velocity $\bar{v}_f \in \mathbb{R}^3$; the initial position and speed $\bar{r}_0 \in \mathbb{R}^3$, $\bar{v}_0 \in \mathbb{R}^3$ are assigned as well, along with the time of flight $\bar{t}_f \in \mathbb{R}$. Vehicle is subject to gravitational acceleration $g \in \mathbb{R}^3$ and to linear drag, with constant coefficient $k_d \in \mathbb{R}_+$. Attitude dynamics is ignored, as characterized by higher bandwidth with respect to the translational one. Therefore, acceleration $u \in \mathbb{R}^3$ constitutes the only control variable. State and control matrices and external disturbances are thus time-invariant and are reported as follows

$$A_c = \begin{bmatrix} \mathbf{0}_{3\times3} & \boldsymbol{I}_{3\times3} \\ \mathbf{0}_{3\times3} & -k_d\boldsymbol{I}_{3\times3} \end{bmatrix}, \quad A = e^{(t_f/N)A_c}$$

$$B_c = \begin{bmatrix} \mathbf{0}_{3\times3} & \mathbf{0}_{3\times1} \\ \boldsymbol{I}_{3\times3} & \mathbf{0}_{3\times1} \end{bmatrix}, \quad B = \int_0^{t_f/N} e^{tA_c}\mathrm{d}t\, B_c$$

$$w_c = \begin{bmatrix} \mathbf{0}_{3\times1} \\ g \end{bmatrix}, \quad w_i = \int_0^{t_f/N} e^{tA_c}\mathrm{d}t\, w_c$$

Finite and non-null bounds on acceleration magnitude $\rho_{\min}, \rho_{\max}$ grant sufficient margin for the attitude controller; a maximum tilt angle $\varphi_{\max}$ with respect to vector ξ further limits the feasible control set [17]. Data are summarized in table I.

TABLE I: Numerical example data

Physical quantity	Value†
$\bar{r}_0, \bar{v}_0$	$[0.5, 0.45, 1.0], [-1.6, 0, 0.6]$
$\bar{r}_f, \bar{v}_f$	$[0, 0, 0], [0, 0, 0]$
$\bar{t}_f$	4.7
g	$[0, 0, -1]$
$k_d, \rho_{\min}, \rho_{\max}$	$0.05, 1.2, 1.6$
$\varphi_{\max}, \xi$	$60°, [0, 0, 1]$

† Normalized according to unitary initial height and gravity acceleration

We seek to reach the final state from the initial one, in the given time of flight and with control subject to mentioned constraints, while minimizing the control magnitude integral. Therefore, with respect to notation outlined in section II, $l_i(\sigma_i) := |\sigma_i|$.

The problem is solved using pointing constraints expressions from both P3 and P4. The optimal trajectory from solution of P4 is reported in Fig. 2a: the obtained control profile shows an initial shutdown period; the crossrange component of the control is visibly lower with respect to the upwards and downrange-oriented ones.

Furthermore, Fig. 2b compares the slack variable with the effective acceleration norm: consistently with definitions in section III, LCvx is validated at each node except for one. Further numerical experiments led on the problem, not reported for page limits, confirm LCvx is violated only at one node, placed during the control magnitude rise between

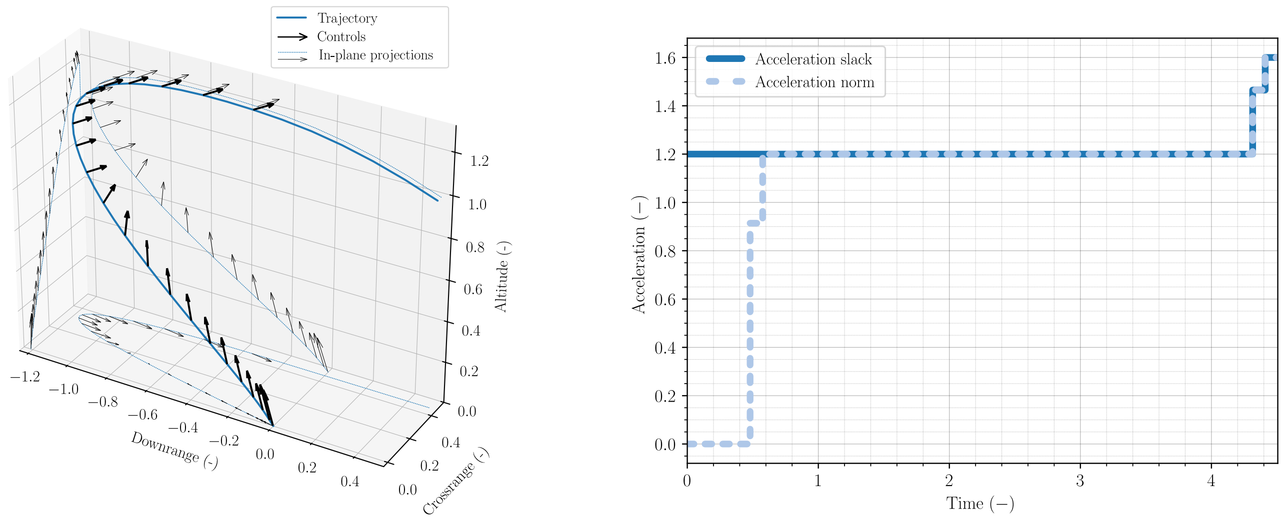

(a) Landing trajectory

(b) Comparison of acceleration slack and acceleration magnitude

Fig. 2: Results for the numerical experiment with pointing constraint from P4

the null and minimum value. Said violation is consistent with previous literature on LCvx.

The examined landing problem is instead infeasible for the pointing constraint of $P3$. The exactly discretized problem is convex, thus the infeasibility certificate obtained for $P3$ certifies that constraints of the original optimal control problem are too restrictive. On the other hand the feasibility basin of the initial problem is widened by allowing engine shut-off using the pointing constraint from $P4$.

V. Conclusion

This paper investigated Discrete Lossless Convexification (DLCvx) for optimal control problems with pointing constraints. We introduced a new formulation that addresses mixed-integer control scenarios, where the control can either be turned off or confined within a specific annular sector. Theoretical guarantees were established for both the classical and the new pointing constraints. Specifically, under the assumptions of transversality, Slater's condition, and controllability, DLCvx for the classical pointing constraint ensures that the original constraints are violated at no more than $n_x - 1$ grid points, while the novel approach guarantees violations at no more than $2n_x - 2$ grid points. These theoretical results enhance the reliability of DLCvx methods in practical applications. At last, both pointing constraints were tested on a landing scenario. The new pointing constraint was shown to expand the feasible set for the landing problem, relative to the classical pointing constraint.

References

[1] Nesterov, Y. and Nemirovskii, A., *Interior-Point Polynomial Algorithms in Convex Programming*. Society for Industrial and Applied Mathematics, 1994.

[2] B. Açıkmeşe and S. Ploen, "Convex programming approach to powered descent guidance for mars landing," *Journal of Guidance, Control, and Dynamics*, vol. 30, no. 5, pp. 1353–1366, 2007.

[3] L. Blackmore, B. Açikmeşe, and D. P. Scharf, "Minimum-landing-error powered-descent guidance for mars landing using convex optimization," *Journal of Guidance, Control, and Dynamics*, vol. 33, no. 4, pp. 1161–1171, Jul. 2010.

[4] S. Kunhippurayil, M. W. Harris, and O. Jansson, "Lossless convexification of optimal control problems with annular control constraints," *Automatica*, vol. 133, p. 109 848, 2021.

[5] B. Acikmese, J. M. Carson, and L. Blackmore, "Lossless convexification of nonconvex control bound and pointing constraints of the soft landing optimal control problem," *IEEE Transactions on Control Systems Technology*, vol. 21, no. 6, pp. 2104–2113, Nov. 2013.

[6] M. W. Harris and B. Açıkmeşe, "Lossless convexification for a class of optimal control problems with linear state constraints," in *52nd IEEE Conference on Decision and Control*, IEEE, 2013, pp. 7113–7118.

[7] M. W. Harris and B. Açıkmeşe, "Lossless convexification of non-convex optimal control problems for state constrained linear systems," *Automatica*, vol. 50, no. 9, pp. 2304–2311, 2014.

[8] D. Malyuta and B. Açikmeşe, "Lossless convexification of optimal control problems with semi-continuous inputs," *IFAC-PapersOnLine*, vol. 53, no. 2, pp. 6843–6850, 2020.

[9] M. W. Harris, "Optimal control on disconnected sets using extreme point relaxations and normality approximations," *IEEE Transactions on Automatic Control*, vol. 66, no. 12, pp. 6063–6070, 2021.

[10] R. Yang and X. Liu, "Convex hull relaxation of optimal control problems with general nonconvex control constraints," *IEEE Transactions on Automatic Control*, vol. 69, no. 6, pp. 4028–4034, Jun. 2024.

[11] K. Echigo, C. R. Hayner, A. Mittal, S. B. Sarsilmaz, M. W. Harris, and B. Açıkmeşe, "Linear programming approach to relative-orbit control with element-wise quantized control," *IEEE Control Systems Letters*, vol. 7, pp. 3042–3047, 2023.

[12] D. Malyuta, T. P. Reynolds, M. Szmuk, *et al.*, "Convex optimization for trajectory generation: A tutorial on generating dynamically feasible trajectories reliably and efficiently," *IEEE Control Systems Magazine*, vol. 42, no. 5, pp. 40–113, 2022.

[13] D. Luo, K. Echigo, and B. Açıkmeşe, "Revisiting lossless Convexification: Theoretical guarantees for discrete-time optimal control problems," *arXiv [math.OC]*, 2024.

[14] J. Borwein and A. Lewis, *Convex Analysis and Nonlinear Optimization*. Springer, 2006.

[15] H. Bauschke, *Convex analysis and monotone operator theory in hilbert spaces*, 2011.

[16] F. Clarke, *Functional Analysis, Calculus of Variations and Optimal Control*. Springer, 2013, vol. 264.

[17] M. Szmuk, C. A. Pascucci, D. Dueri, and B. Acikmese, "Convexification and real-time on-board optimization for agile quad-rotor maneuvering and obstacle avoidance," in *2017 IEEE/RSJ IROS*, IEEE, Sep. 2017.